

Nucleophilic Addition to π-Allyl Gold(III) Complexes: Evidence for Direct and Undirect Paths

Jessica Rodriguez, Marte Sofie Martinsen Holmsen, Yago García-Rodeja, E. Daiann Sosa Carrizo, Pierre Lavedan, Sonia Mallet-Ladeira, Karinne Miqueu, Didier Bourissou

▶ **To cite this version:**

Jessica Rodriguez, Marte Sofie Martinsen Holmsen, Yago García-Rodeja, E. Daiann Sosa Carrizo, Pierre Lavedan, et al.. Nucleophilic Addition to π-Allyl Gold(III) Complexes: Evidence for Direct and Undirect Paths. Journal of the American Chemical Society, 2021, 143 (30), pp.11568-11581. 10.1021/jacs.1c04282 . hal-03336159

HAL Id: hal-03336159
https://univ-pau.hal.science/hal-03336159

Submitted on 15 Nov 2021

HAL is a multi-disciplinary open access archive for the deposit and dissemination of scientific research documents, whether they are published or not. The documents may come from teaching and research institutions in France or abroad, or from public or private research centers.

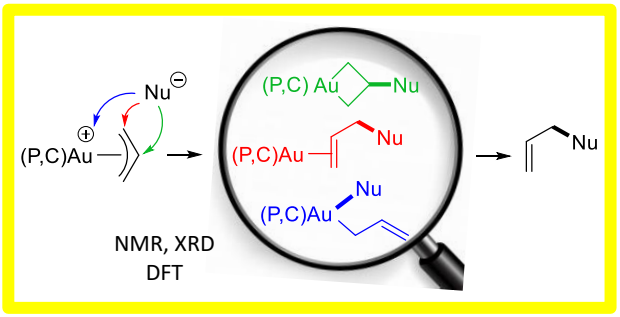
L'archive ouverte pluridisciplinaire **HAL**, est destinée au dépôt et à la diffusion de documents scientifiques de niveau recherche, publiés ou non, émanant des établissements d'enseignement et de recherche français ou étrangers, des laboratoires publics ou privés.

Nucleophilic Addition to π-Allyl Gold(III) Complexes: Evidence for Direct and Undirect Paths

Jessica Rodriguez,[†] Marte Sofie Martinsen Holmsen,[†] Yago García-Rodeja, E. Daiann Sosa Carrizo, Pierre Lavedan, Sonia Mallet-Ladeira, Karinne Miqueu* and Didier Bourissou*

[†]These authors contributed equally.

ABSTRACT: π-Allyl complexes play a prominent role in organometallic chemistry and have attracted considerable attention, in particular the π-allyl Pd(II) complexes which are key intermediates in the Tsuji-Trost allylic substitution reaction. Despite the huge interest for π-complexes of gold, π-allyl Au(III) complexes were only authenticated very recently. Herein, we report the reactivity of (P,C)-cyclometallated Au(III) π-allyl complexes towards β-diketo enolates. Behind an apparently trivial outcome, *ie* the formation of the corresponding allylation products, meticulous NMR studies combined with DFT calculations revealed a complex and rich mechanistic picture. Nucleophilic attack can occur at the central and terminal positions of the π-allyl as well as the metal itself. All paths are observed and are actually competitive, whereas addition to the terminal positions largely prevails for Pd(II). Auracyclobutanes and π-alkene Au(I) complexes were authenticated spectroscopically and crystallographically, Au(III) σ-allyl complexes were unambiguously characterized by multi-nuclear NMR spectroscopy. Nucleophilic additions to the central position of the π-allyl and to gold are reversible. Over time, the auracyclobutanes and the Au(III) σ-allyl complexes evolve into the π-alkene Au(I) complexes and release the C-allylation products. The relevance of auracyclobutanes in gold-mediated cyclopropanation was demonstrated by inducing C–C coupling with iodine. The molecular orbitals of the π-allyl Au(III) complexes were analyzed in-depth and the reaction profiles for the addition of β-diketo enolates were thoroughly studied by DFT. Special attention was devoted to the regioselectivity of the nucleophilic attack, but C–C coupling to give the allylation products was also considered to give a complete picture of the reaction progress.



Introduction

π-Allyl transition metal complexes are prominent compounds in organometallic chemistry. They are key intermediates in several major transformations, in the first place the Pd-catalyzed allylic substitution (the Tsuji-Trost reaction).[1] As a result, a number of fundamental studies have been performed on the structure and reactivity of π-allyl complexes, with palladium in particular. Accordingly, their η^1/η^3 coordination isomerism as well as the mechanisms of nucleophilic addition to the π-coordinated allyl ligands are nowadays classics in organometallic chemistry textbooks.[2] Most common is the outer-sphere attack at the terminal position of the π-allyl (Figure 1, path 1), leading to π-alkene complexes and ultimately to allylation products. Numerous and thorough studies have been carried out to decipher the underlying factors, to rationalize the observed products, and to enhance synthetic performance. In particular regio- and stereo-selectivity have attracted considerable attention when dealing with unsymmetrical π-allyl Pd(II) complexes and chiral ligands. A recognized alternative scenario is the attack at the metal itself (path 2), leading to σ-allyl complexes that can then evolve further by reductive elimination to release the allylation products. Although this inner-sphere path has not been observed directly with palladium to our knowledge, its involvement is commonly inferred from the stereochemical outcome of the allylic substitution (retention/inversion of configuration of the allylic substrates depending on the hard/soft nature of the nucleophile).[2] In addition, computations have found the inner-sphere path as the lowest energy mechanism in some allylic substitutions.[3] A third possibility for the nucleophile, which remains a chemical curiosity, consists in the outer-sphere attack at the central position of the π-allyl (path 3), leading to a metallacyclobutane derivative. This path was first authenticated in 1977 by Green *et al* in the reaction of cationic $Cp_2M(\pi\text{-allyl})$ complexes (M = Mo, W) with hydrides and strong carbon nucleophiles.[4] Later on, it was also observed by Bergmann and Stryker from the reaction of $Cp^*(L)M(\pi\text{-allyl})$ complexes (M = Ir, Rh) with enolates.[5] It is extremely scarce in palladium chemistry where nucleophilic attack at the terminal carbon atoms very much prevails, but the formation of palladacyclobutanes was found to be favored in a few specific systems.[6] Of note, the metallacyclobutanes may evolve to give cyclopropane derivatives, as substantiated occasionally with Ir, Rh and Pd.[5c,6d]

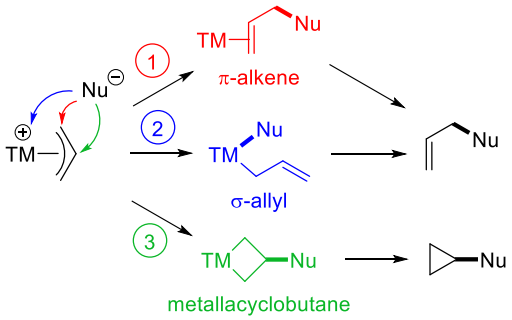


Figure 1. Possible reactive sites for the addition of nucleophiles to π-allyl complexes.

The advent of gold-catalyzed π-activation has stimulated huge interest for gold π-complexes over the past three decades.[7] Nevertheless, it was not until 2020 that π-allyl Au(III) complexes were isolated and well characterized. Two parallel studies were carried out by the Tilset group[8] and our group[9] on complexes **1** and **2/2'**, respectively (Figure 2).[10] The π-allyl ligand is asymmetrically coordinated and highly fluxional in the (N,C)-cyclometallated complex **1**. In contrast, it is quasi-symmetrically coordinated, rigid and highly delocalized in the (P,C)-cyclometallated complexes **2** and **2'**.

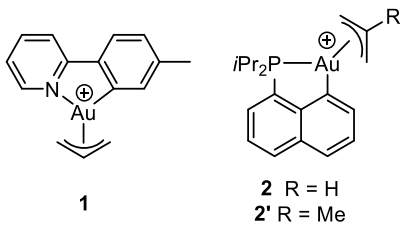
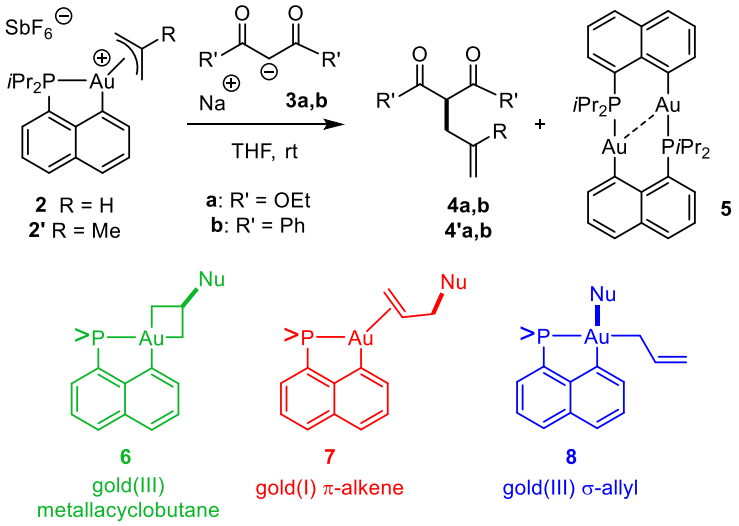


Figure 2. First π-allyl Au(III) complexes authenticated.

Taking advantage of the availability and stability of complexes **2** and **2'** (no sign of degradation detected after days of storage at room temperature under air), their reactivity towards nucleophiles was assessed.[9] π-Coordination of the allyl moiety to Au(III) was found to mediate nucleophilic additions of β-diketo enolates **3a,b** to give the corresponding C–C coupling products **4/4'a,b** (Scheme 1). The close analogy with related Pd chemistry prompted us to carry out detailed mechanistic studies on these reactions. As reported hereafter, behind an apparently trivial outcome, meticulous NMR studies combined with DFT calculations revealed a complex and rich mechanistic picture for the allylation of β-diketo enolates mediated by Au(III). Au(III) metallacyclobutane complexes **6**, π-alkene Au(I) complexes **7** as well as Au(III) σ-allyl complexes **8** were authenticated, providing direct evidence for nucleophilic addition of β-diketo enolates to all three reactive sites of the π-allyl Au(III) complexes, *ie* the central and terminal carbon atoms (outer-sphere paths) as well as gold itself (inner-sphere path). The formation of Au(III) metallacyclobutane complexes **6** and Au(III) σ-allyl complexes **8** proved reversible, evolving over time to the π-alkene Au(I) complexes **7** and ultimately to the C-allylation products **4**. The electronic structure of the π-allyl Au(III) complexes **2** and **2'** has been analyzed in-depth and compared to that of an analogous Pd complex, providing rationale for the existence of three competitive sites for the addition of nucleophiles in the case of gold. The reaction profiles for the addition of β-diketo enolates have also been computed by DFT, giving more insight into the factors dictating the favored reaction sites and the progress of the reaction. In addition, the relevance of Au(III) metallacyclobutanes in gold-mediated cyclopropanation has been demonstrated by inducing C–C coupling from **6** before it evolves to the π-alkene complex **7**.



Scheme 1. Reactions of the (P,C)-cyclometallated π-allyl Au(III) complexes **2/2'** with β-diketo enolates **3a,b** studied in this work, with the three possible complexes **6-8** originating from nucleophilic attack at the central or terminal position of the π-allyl or at gold.

Results and discussion

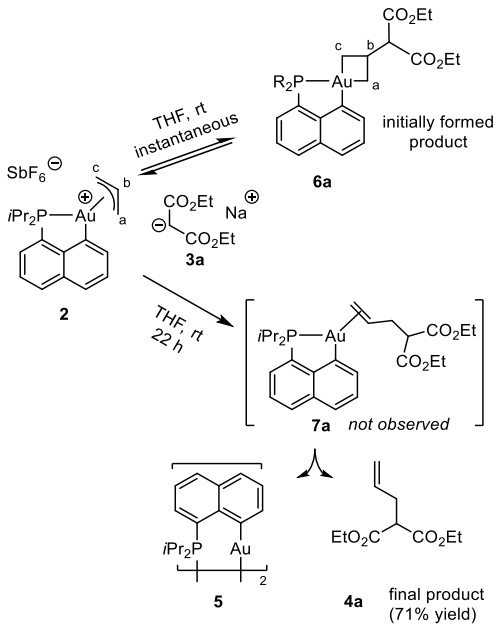
Part I. Mechanistic investigations of nucleophilic additions to π-allyl complexes 2 and 2' by NMR spectroscopy

With the aim to detect some intermediates on the way to the C-allylation products **4/4'a,b**, the reactions of complexes **2** and **2'** with the β-diketo enolates **3a,b** were monitored by ^{31}P and ^{1}H NMR spectroscopy right after mixing. Among the four studied reactions, **2** + **3b** and **2'** + **3a** led to intricate mixtures difficult to decipher (*vide infra*). The reactions **2** + **3a** and **2'** + **3b** were more clear-cut. In both cases, we observed essentially one type of intermediate gold complex that we could isolate and identify. Note that after 4-22 hours at room temperature, all the four coupling reactions lead to the C-allylation products (**4/4'a,b**, 71-99% yield) along with the Au(I) dimer **5**.[9]

Reaction 2 + 3a: reversible formation of an auracyclobutane

Treatment of the π-allyl Au(III) complex **2** with a stoichiometric amount of sodium diethylmalonate **3a** instantaneously led to the formation of one major product (85% spectroscopic yield). After work-up, this compound was isolated as a yellowish solid in 52% yield. The new complex was unambiguously authenticated by multinuclear NMR spectroscopy as the auracyclobutane complex **6a**, resulting from nucleophilic attack at the central position of the π-allyl moiety (Scheme 2, top). The ^{31}P NMR signal of **6a** is found at δ 62.3 ppm, upfield by 26 ppm compared to that of **2**. Formation of the auracyclobutane is apparent from the large shielding of the H_a (δ 0.76 and 1.50), H_c (δ 0.14 and 1.25), C_a (δ 4.2, J_{PC} 95.7 Hz) and C_c (δ −14.5, J_{PC} 5.7 Hz) resonances (Figure 3, top).[5a,5c,11] The very good match of the experimental data for **6a** (^1H, ^{13}C chemical shifts, J_{PC} coupling constants) with those obtained computationally (Table S3)[12] corroborates our structural assignment. Note that we are aware of only one example of an auracyclobutane which was reported by Dinger and Henderson in 1999.[13] It was prepared by a completely different route, *ie* reaction of a cyclometallated (N,C)Au(III)Cl_2 complex with Ag_2O and tetracyanocyclopropane. Unfortunately, the presence of four cyano substituents on the carbon atoms bonded to gold prevents comparison of its NMR pattern with that of complex **6a**.

The auracyclobutane **6a** is quite unstable and evolves over time to form the Au(I) dimer **5** and release the coupling product **4a** (22 h, 71% yield). This transformation most likely involves the π-alkene complex **7a** as a key unobserved intermediate (Scheme 2, bottom). We surmise that nucleophilic addition to the central carbon atom of the π-allyl ligand is kinetically favored and reversible. Accordingly, the metallacyclobutane **6a** would be initially formed, and then evolve over time towards the π-alkene complex **7a** by nucleophilic attack of the malonate **3a** at the terminal positions of the π-allyl complex **2**.



Scheme 2. Reactivity of the π-allyl Au(III) complex **2** with enolate **3a**, reversibility of the nucleophilic attack at the central position of the π-allyl.

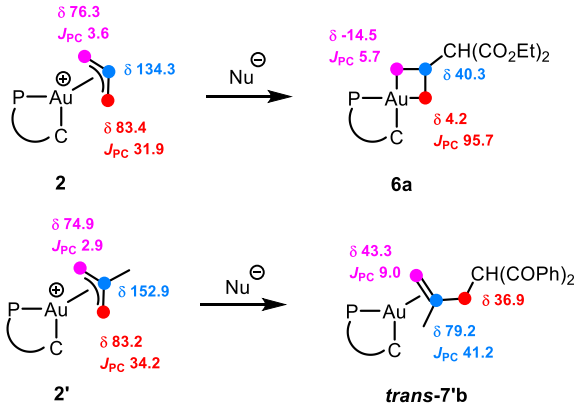
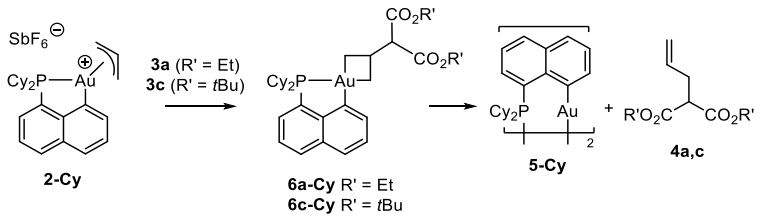
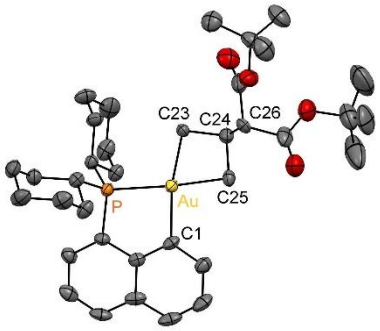


Figure 3. Diagnostic ^{13}C NMR resonances for the allyl fragment in the π-allyl complexes **2/2'**, auracyclobutane **6a** and π-alkene complex **7'b** (data in d_8-THF, chemical shifts in ppm, coupling constants in Hz).

Unfortunately, we were not able to obtain crystals of **6a** suitable for X-ray diffraction analysis. In order to impart higher crystallinity, we changed the substituents at phosphorus from isopropyl to cyclohexyl. The corresponding π-allyl Au(III) complex **2-Cy** was reacted with diethyl malonate **3a** (Scheme 3, top).[12] The reaction worked well and cleanly afforded the corresponding auracyclobutane **6a-Cy**. Attempts to crystallize this complex remained unsuccessful, only the ensuing gold(I) dimer **5-Cy** could be analyzed by X-ray diffraction analysis.[12] Gratifyingly, reacting di-*tert*-butyl malonate **3c** with **2-Cy** turned out to cleanly afford the auracyclobutane **6c-Cy** and crystals suitable for X-ray diffraction analysis could be obtained in this case by layering a fluorobenzene solution of **6c-Cy** with pentane at −25 °C (Scheme 3, bottom).[12] The gold center is in a square planar environment, as expected for a Au(III) complex. The C1–Au–P chelating angle of 82.98(16)° deviates slightly from the ideal 90° value, whereas the C23–Au–C25 angle within the four-membered ring is strongly bent at 68.5(3)°. The auracyclobutane ring adopts a quasi-planar diamond shaped geometry [the C23AuC25 and C23C24C25 planes are folded by only 5.1(9)°]. The C23–C24 and C24–C25 bonds [1.555(9) and 1.543(9) Å, respectively] are much longer than in the Au(III) π-allyl complexes **2** and **2'** (1.38-1.42 Å),[9] and are now clearly single bonds. The newly-formed C24–C26 bond is also typical for a $C(sp^3)$-$C(sp^3)$ bond at 1.524(9) Å. We found only one precedent for a crystallographically-characterized metallacyclobutane featuring a malonate substituent.[5g] It is an Ir(III) species deriving from a π-cinnamyl ($PhCHCHCH_2$) complex. The four-membered ring is also quasi planar, and the C–C bond formed by nucleophilic attack at the central position is similar at 1.558(6) Å. The formation of **6a,c-Cy** shows that nucleophilic addition to the central position of the π-allyl is not limited to the reaction **2** + **3a** and is in fact quite favored for Au(III) π-allyl complexes.

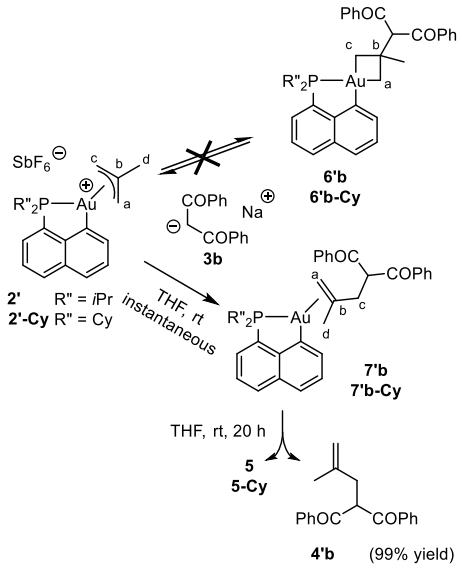




Scheme 3. Formation of auracyclobutanes **6a,c-Cy**. Molecular structure of the Au(III) auracyclobutane **6c-Cy** (hydrogen atoms omitted for clarity, ellipsoids shown at 50% probability). Selected bond lengths (Å) and angles (°): Au–C25 2.086(7), Au–C23 2.111(7), C24–C25 1.543(9), C23–C24 1.555(9), C24–C26 1.524(9), C23–Au–C25 68.5(3), C1–Au–P 82.98(16), C23–C24–C25 99.4(5).

Reaction 2' + 3b: formation of a (P,C)-cyclometallated Au(I) π-alkene complex

NMR monitoring of the reaction between the π-methallyl Au(III) complex **2'** and the β-diketo enolate **3b** (Scheme 4) also showed the instantaneous formation of one major complex (82% spectroscopic yield). Upon work-up, this product was isolated in 56% yield. It shows a ^{31}P NMR signal at δ 58.1 ppm, very close to that of the auracyclobutane complex **6a**. However, the ^{1}H and ^{13}C NMR signatures for the two species are markedly different, suggesting that nucleophilic attack did not occur at the central position of the π-allyl to give **6'b** in this case. Complete NMR characterization at −30 °C enabled to assign all signals unequivocally.[12] Most diagnostic is the shielding of the C_a and C_c resonances with respect to the π-allyl precursor **2'** (Figure 3, bottom), but to a much lesser extent than that observed for the auracyclobutane **6a**. These data made us envision the formation of the π-alkene complex **7'b** by nucleophilic attack at the terminal positions of the π-methallyl. To confirm this hypothesis, the NMR data for **7'b** were computed and a very good agreement was found with those determined experimentally (Table S7).[12] Complex **7'b** is unstable and leads with time to the formation of the C-allylation product **4'b** together with the Au(I) dimer **5** (20 h, 99% yield).



Scheme 4. Reactivity of π-allyl Au(III) complexes **2'**/**2'-Cy** with β-diketo enolate **3b**.

Since crystals of **7'b** suitable for X-ray diffraction analysis could not be obtained, we again turned to the PCy_2-substituted system. The corresponding π-methallyl complex **2'-Cy** reacted similarly with enolate **3b**. The ensuing π-alkene complex **7'b-Cy** was obtained in >98% spectroscopic yield and fully characterized.[12] Gratifyingly, crystals of suitable quality could be grown in this case by layering pentane over a diethylether solution of **7'b-Cy** at 6 °C (Figure 4). Accordingly, the gold center is in a trigonal planar environment. The alkene is η^2-coordinated to gold with almost identical Au–C bond lengths [Au–C23 2.144(5) and Au–C24 2.158(4) Å]. Of note, the alkene sits in the coordination plane of gold [the PAuC1 and C23AuC24 planes are tilted by only 6.6(4)°], despite the associated steric shielding. This suggest significant Au→π*(C=C) backdonation, as also apparent from the noticeable elongation of the C=C bond (1.420(9) Å *versus* 1.339 Å in the free alkene). Gold(I) π-complexes are presumed to be key intermediates in a number of catalytic transformations and have therefore attracted considerable attention. Among stable π-alkene Au(I) complexes, compounds **7'b** and **7'b-Cy** represent rare examples of neutral species. They are tricoordinate, but does not involve chelating (N,N) or (P,N) ligands as is the case for known examples.[7e] In fact, compounds **7'b** and **7'b-Cy** represent the first cyclometallated π-alkene Au(I) complexes.

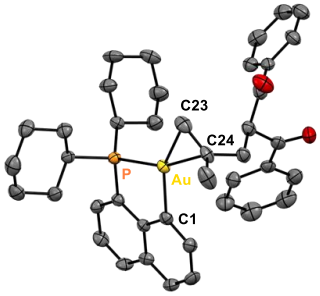


Figure 4. Molecular structure of the π-alkene Au(I) complex **7'b-Cy** (hydrogen atoms omitted for clarity, ellipsoids shown at 50% probability). Selected bond lengths (Å) and angles (°): Au–C23 2.144(5), Au–C24 2.158(4), C23-C24 1.420(9), P-Au-C23 122.9(2), P-Au-C24 160.6(2), C1-Au-C23 152.6(2), C1-Au-C24 114.1(2), P-Au-C1 84.3(1).

Of note, complete NMR characterization of **7'b-Cy** in solution at –20 °C revealed the presence of two isomers, referred as ***trans*-7'b-Cy** and ***cis*-7'b-Cy** (Figure 5, top), in a 10/1 ratio. The major form corresponds to that observed in the solid state, with the CH_2 end *cis* to the PCy_2 group. The ^{13}C olefinic resonances of **7'b-Cy** are significant shielded compared to those of the free alkene **4'b**, further supporting strong Au→π*(C=C) backdonation and considerable metallacyclopropane character in **7'b-Cy**. At 25 °C, the ^1H NMR resonances of ***trans*-7'b-Cy** and ***cis*-7'b-Cy** are significantly broadened, suggesting fluxional behavior and/or interconversion of the two isomers on the NMR time scale. This was further supported by ^{31}P-^{31}P EXSY experiments where exchange between ***trans*-7'b-Cy** and ***cis*-7'b-Cy** was observed at –10 °C (Figure 5, bottom).[12]

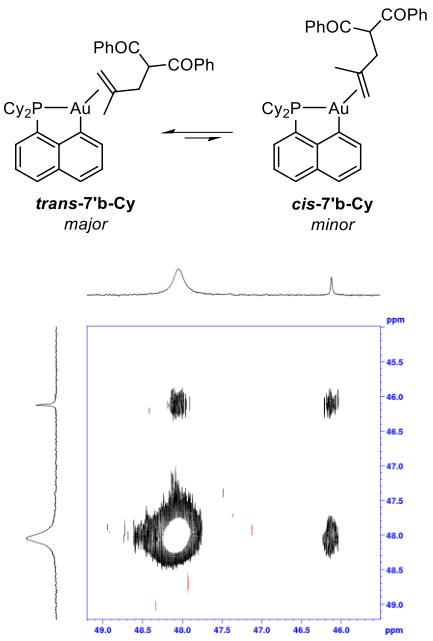
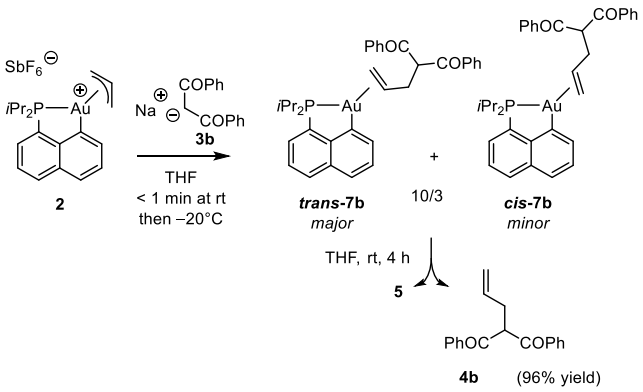


Figure 5. *Trans* and *cis* isomers of the π-alkene Au(I) complex **7'b-Cy** and ^{31}P-^{31}P EXSY spectrum (202.45 MHz, CD_2Cl_2, –10 °C, mixing time 250 ms) substantiating their interconversion.

Back to reactions 2 + 3b and 2' + 3a: nucleophilic attack at the allyl moiety versus gold

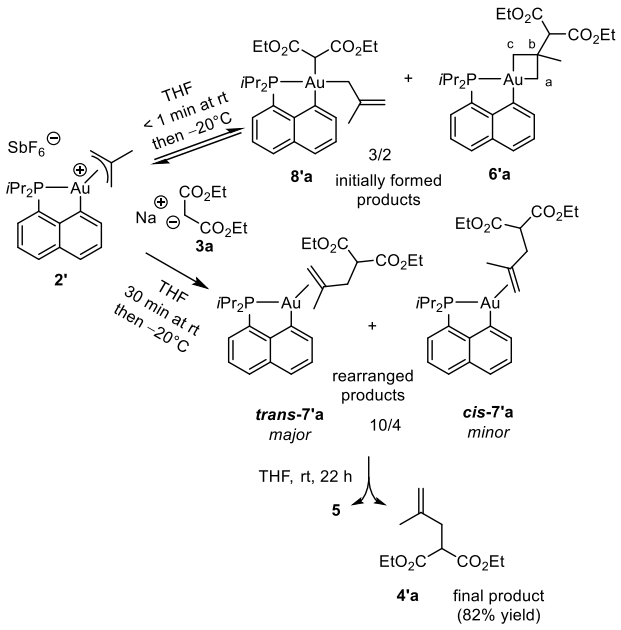
Having unambiguously identified auracyclobutanes and π-alkene Au(I) complexes as intermediates in the previous reactions, we tried to take advantage of this knowledge to decipher the complex mixtures obtained in the two other reactions **2** + **3b** and **2'** + **3a**. Mixing **2** and **3b** at room temperature immediately followed by cooling to –20 °C provided a reaction mixture much easier to analyze (Scheme 5). It contains two analogous species identified as the *trans* and *cis* forms of the π-alkene Au(I) complex **7b** (10/3 ratio). At room temperature, these compounds rapidly evolve to release the C-allylation product **4b** (4 h, 96% yield).



Scheme 5. Reactivity of the π-allyl Au(III) complex **2** with β-diketo enolate **3b**.

Finally, the reaction **2'** + **3a** was also reinvestigated by cooling the reaction mixture immediately after mixing. This proved to be the most complex but also the most interesting case (Scheme 6). Initially, two species were observed in a 3/2 ratio. The minor one was authenticated as the auracyclobutane **6'a** based on its very diagnostic shielded $AuCH_2$ resonances (C_a δ 15.7 J_{PC} 93.7 Hz, C_c δ –2.8 J_{PC} 5.3 Hz). The major species proved to be the σ-allyl Au(III) complex **8'a**. Its structure was unambiguously ascertained by multinuclear NMR spectroscopy. In short, (*i*) the ^1H and ^{13}C NMR resonances for the σ-methallyl part are very similar to those of the direct precursor of **2'**, *ie* the (P,C)AuI(σ-methallyl) complex,[9] (*ii*) ^1H-^{31}P HMBC experiment shows a correlation between the phosphorus and C*H*$(CO_2Et)_2$ signals (Figure S31), and

(*iii*) the experimental and computed NMR data are in very good agreement (Table S8).[12] The formation of **8'a** provides for the first time evidence for nucleophilic attack at gold. In line with the stronger *trans* influence of carbon *versus* phosphorus,[14] the incoming malonate is introduced preferentially and actually selectively in the position *trans* to naphthyl. Upon warming the mixture of σ-allyl Au(III) complex **8'a** and auracyclobutane **6'a** to 25 °C for *ca* 30 min and cooling again to –20 °C, a completely different ^{31}P NMR spectrum was obtained (Figure 6). Quantitative conversion into the π-alkene Au(I) complex **7'a** was apparent, with the *trans* and *cis* forms again coexisting (10/4 ratio). Thus, addition to the central position of the methallyl as well as to gold is reversible and over time, the reaction evolves towards nucleophilic attack at the terminal positions. Finally, the C-allylation product **4'a** is slowly released from the π-alkene Au(I) complex **7'a** at room temperature (22 h, 82% yield) with concomitant formation of the Au(I) dimer **5**.



Scheme 6. Reactivity of the π-allyl Au(III) complex **2'** with enolate **3a**.

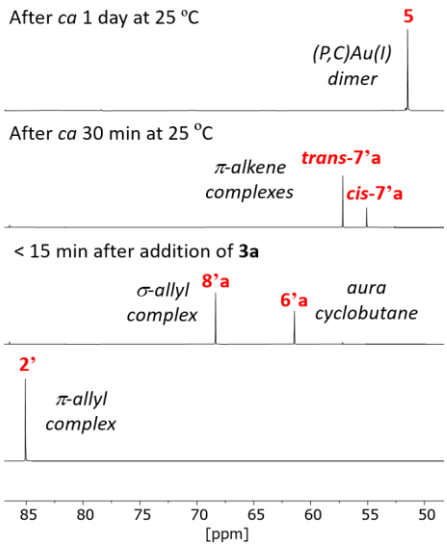


Figure 6. Stacked ^{31}P NMR spectra showing the progress of the reaction between the π-allyl Au(III) complex **2'** and enolate **3a** in d_8-THF (Top: at 25 °C and 121.49 MHz, otherwise: at −20 °C and 202.45 MHz).

Part II. Mechanistic investigations of nucleophilic additions to π-allyl complexes 2 and 2' by DFT calculations

With the aim to better understand and rationalize the experimental results, the electronic structure of the Au(III) π-allyl complexes **2/2'** and their reactivity towards β-diketo enolates were investigated in detail by Density Functional Theory (DFT). Calculations were performed at the SMD(THF)-B3PW91/SDD+f(Au),6-31G**(other atoms) level of theory.

Electronic structure of the Au(III) versus Pd(II) π-allyl complexes

The η^3 quasi-symmetric coordination of the allyl moiety in the Au(III) complexes [(P,C)Au(π-allyl/π-methallyl)]$^+$ **2/2'** was previously established by NMR and crystallographic data as well as DFT calculations.[9] Here, the electronic properties of these π-allyl complexes (atomic charges, Molecular Orbitals) were thoroughly analyzed, with respect to the possible sites for nucleophilic addition to occur (terminal and/or central position of the allyl moiety, gold itself). The analogous [$(Ph_3P)_2$Pd(π-allyl)]$^+$ complex **2-Pd** was also considered to shed light into the peculiar properties of the Au(III) complexes and their ability to afford Au(III) metallacyclobutanes **6**, π-alkene Au(I) complexes **7** as well as Au(III) σ-allyl complexes **8**. The regioselectivity of nucleophilic additions to π-allyl complexes, in particular Pd(II) species has attracted much attention computationally. Early pioneering studies by Curtis and Eisenstein pointed out the major role of frontier orbitals (as opposed to atomic charges) and identified the factors responsible for the preference of nucleophiles to attack the terminal positions of $L_3(OC)_2$Mo(II)(π-allyl) complexes.[15] Further theoretical investigations by Mealli and Musco refined the description and analysis of the frontier orbitals of π-allyl complexes in the case of nucleophilic additions to [$(H_3P)_2$M(π-allyl)]$^+$ (M = Pd, Pt) complexes.[16] More recently, reaction profiles of several Pd-catalyzed allylation reactions have been theoretically investigated considering both the inner- and outer-sphere paths.[3,17]

The atomic charges of the Au(III) complexes **2/2'** and Pd(II) complex **2-Pd** were computed and compared (Table S2).[12] The positive charge is borne by the metal fragment, (P,C)Au or $(Ph_3P)_2$Pd. It is highly concentrated on gold in **2** and **2'** [*q*(Au) = 0.88] but more delocalized in **2-Pd** [*q*(Pd) = 0.29]. For the allyl moiety, very similar situations were found for the three complexes, with minor differences between the terminal and central positions. The charges of the terminal CH_2 and central CH/CMe groups are in fact all close to zero as well as the total charge of the allyl/methallyl moiety. The fact that Au(III) complexes **2** and **2'** readily react with nucleophiles at either sites of the π-allyl or at the metal contrasts with the very favored attack at the terminal sites of Pd(II) π-allyl complexes such as **2-Pd**. It is thus unlikely that the reactivity of Au(III) π-allyl complexes is under charge control. In line with previous computational studies,[15,16] frontier orbital control most probably prevails and inspecting the Molecular Orbitals (MO) of the Au(III) and Pd(II) complexes is certainly more relevant.

The MO diagram of the [(P,C)Au(π-allyl)]$^+$ complex **2** was built using the AOMIX program.[18] The molecular orbitals relevant to nucleophilic additions are displayed in Figure 7, left. They arise from the homo (in-plane $5d_{x^2-y^2}$), lumo and lumo+1 orbitals for the (P,C)Au fragment and the vacant π2 / π3 orbitals of the π-allyl cation. The three frontier orbitals of (P,C)Au interact with the non-bonding π2 orbital of the allyl to form the HOMO, LUMO and LUMO+1 of the [(P,C)Au(π-allyl)]$^+$ complex **2**. In the vacant orbitals LUMO and LUMO+1, the largest coefficients on the allyl moiety are found on the terminal positions C_{term}. There is only minor, if any, contribution of the central position C_{cent} but significant participation of the gold atom. Overall, the LUMO and LUMO+1 are relatively similar in shape and close in energy (–1.97 and –1.81 eV, respectively). Interestingly, the LUMO+2 of complex **2** corresponds to a bonding interaction between the anti-bonding orbital π3 of the allyl and the lumo+1 of the (P,C)Au fragment. This orbital sits at –1.38 eV, only 0.4-0.6 eV above the LUMO/LUMO+1. The LUMO+2 has large contribution of the central carbon atom C_{cent} (15.5% *versus* 7.8 / 6.5% on the terminal positions C_{term}) and significant participation of gold (20.3%).[19] The small energy gap found between the three vacant MO of lowest energy combined with the major contributions of C_{term} in LUMO/LUMO+1 and C_{cent} in LUMO+2 are consistent with the possibility for nucleophiles to attack at all sites of the π-allyl of complex **2**. Nucleophilic addition to gold to give Au(III) σ-allyl complexes is also conceivable given the noticeable contribution of the metal in the three vacant orbitals. A very similar situation is met in the corresponding methallyl Au(III) complex

2' (Figures S56 and S57)[12] indicating that the methyl substituent in the central position of the allyl has no huge impact. The LUMO/LUMO+1 of **2'** are slightly raised and brought closer in energy, at –1.81 and 1.75 eV, while the LUMO+2 remains essentially unchanged at –1.32 eV.

A noticeable feature of the gold complexes **2** and **2'** is the low energy of the LUMO+2 with major contribution of the central position C_{cent} of the π-allyl. This may explain why the formation of the metallacyclobutane is competitive with that of the π-alkene complexes in the case of gold. To corroborate this hypothesis, the MO diagram of the related Pd complex $[(Ph_3P)_2Pd(\pi\text{-allyl})]^+$ **2-Pd** was analyzed for comparison (Figure 7, right). It is quite similar to those of **2/2'**, but with some noticeable differences. The LUMO of **2-Pd** results from the anti-bonding interaction between the homo of $[(Ph_3P)_2Pd]$ (in-plane $4d_{x2-y2}$) and the non-bonding π2 orbital of the allyl. It is located at –1.86 eV (very close to that found for **2** and **2'**) with large contributions from the terminal carbon atoms C_{term} (12.3% for each carbon). In stark contrast with that observed for the gold complexes **2** and **2'**, no vacant orbital with significant contribution from the central carbon atom C_{cent} was found before LUMO+15 for **2-Pd**. This vacant orbital results from the bonding interaction between the lumo of $[(Ph_3P)_2Pd]$ and the anti-bonding orbital π3 of the allyl. It has much larger coefficient on C_{cent} than C_{term} (15.2% *versus* 6.4 / 5.8%) but lies high in energy (0.34 eV). Of note, the contribution of the metal is substantially smaller in the LUMO+15 of **2-Pd** (8.3%) than in the LUMO+2 of **2/2'** (20.3 and 18.8%, respectively). In the end, the energy difference between the C_{term} and C_{cent}-centered vacant orbitals is much larger in the Pd(II) than Au(III) complexes (2.2 *versus* 0.4-0.6 eV), in line with the marked preference for nucleophiles to attack Pd complexes at the terminal rather than central position of the π-allyl.

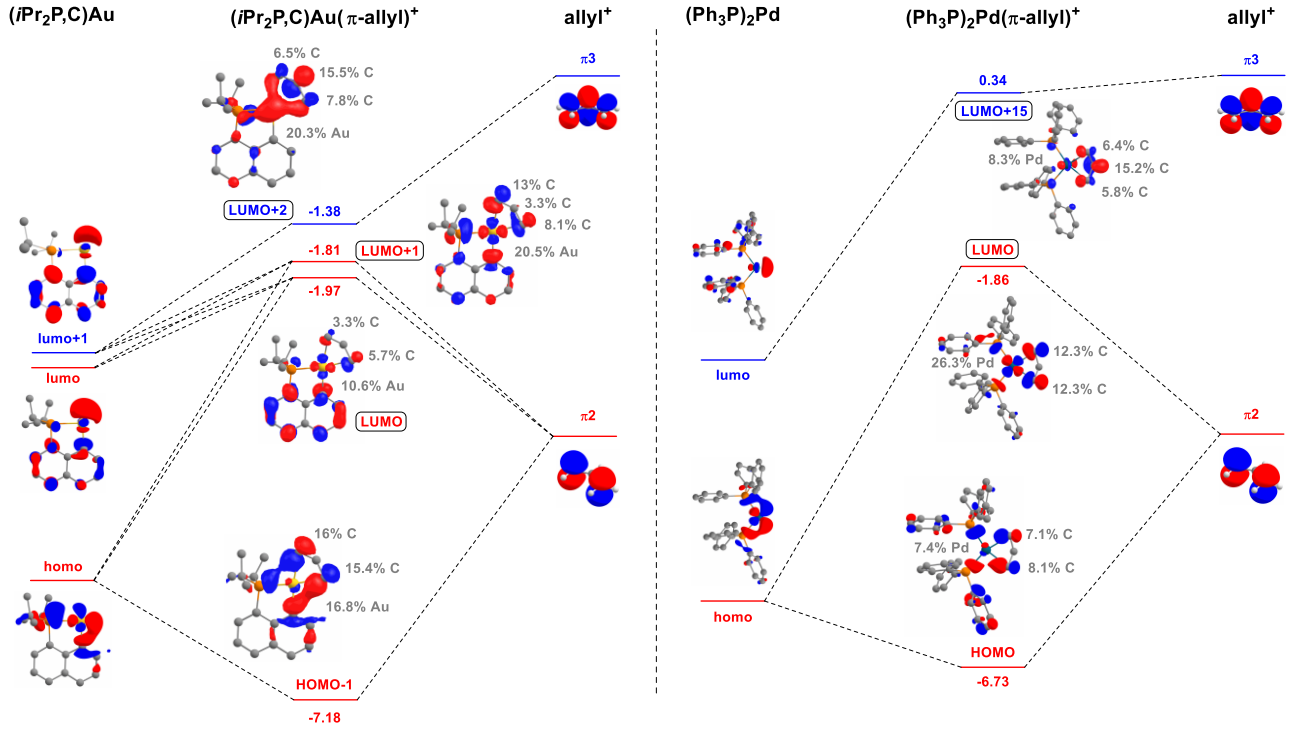


Figure 7. MO diagrams for the Au(III) complex $[(P,C)Au(\pi\text{-allyl})]^+$ **2** (left) and its Pd(II) analog $[(Ph_3P)_2Pd(\pi\text{-allyl})]^+$ complex **2-Pd** (right) showing the vacant orbitals relevant to nucleophilic additions. Energy of the MOs in eV, cutoff: 0.05. Contribution of the main atoms in each MO in %. Red lines correspond to MOs with large contributions on the terminal carbon atoms of the π-allyl moiety while blue lines correspond to MOs with large contributions on the central carbon atom of the π-allyl.

To summarize, inspection of the molecular orbitals revealed noticeable differences between the Au(III) and Pd(II) π-allyl complexes **2/2'** and **2-Pd**. The LUMO (and LUMO+1 in the case of gold) have large contributions on C_{term} in all complexes, but vacant orbitals with significant contributions on C_{cent} are accessible in energy only in the Au(III) complexes, making the formation of auracyclobutanes much more favorable than palladacyclobutanes.

Analyzing the electronic structure of the π-allyl complexes is of course informative but it does not take into account the nucleophile and the way it interacts with the π-allyl complex. To gain more insight into the reactivity of the π-allyl Au(III) complexes with respect to the regioselectivity and reversibility of nucleophilic additions, the energy profiles for the reactions **2** + **3a** and **2'** + **3b** leading to the auracyclobutane **6a** and π-alkene complex **7'b**, respectively were thoroughly investigated, considering and comparing the different possible pathways. Special attention was devoted to the nucleophilic attack of the β-diketo enolate at the π-allyl Au(III) complex, but C–C coupling to give the final allylation products was also considered to have a complete picture of the reaction progress.

The same level of theory SMD(THF)-B3PW91/SDD+f(Au),6-31G**(other atoms) was used throughout. Because of convergence issues in the localization of some of the transition states at the SMD(THF)-B3PW91-D3(BJ) level, dispersion effects were not taken into account. Nonetheless, their impact has been assessed on the the key paths of the first reaction, **2** + **3a**.[12] and no major differences were observed in the energies and geometries. Dispersion does not seem to play a crucial role here.

Energy profile for the reaction 2 + 3a

Nucleophilic additions of diethyl malonate **3a** to the three positions of the π-allyl moiety of complex **2** were first studied (Figure 8). Attack at the central position (transition state **TS1**) is very easy, with an activation barrier $\Delta G^{\neq}$ of only 3.9 kcal/mol, and the formation of the auracyclobutane **6a** is exergonic (ΔG –23.1 kcal/mol). The optimized structure of **6a** (Figure S58)[12] matches well with that determined crystallographically for **6c-Cy**. The largest differences are a slight tilt of the four-membered ring (the angle between the CAuC and CCC planes amounts to 21.1°) and a slightly longer C–CH(CO_2R') bond at 1.539 Å. Low-energy paths were also found for nucleophilic attack of **3a** at the terminal positions of the π-allyl (*trans* to P, **TS2** and *cis* to P, **TS3**) but the corresponding activation barriers ($\Delta G^{\neq}$ 6.3 and 4.9 kcal/mol, respectively) are slightly larger than for the attack at C_{cent}. The ensuing π-alkene Au(I) complexes ***trans*-7a** and ***cis*-7a** are downhill in energy from **2** + **3a** (ΔG –34.2 and –33.7 kcal/mol, respectively) and thus more stable than the auracyclobutane **6a** by about 10 kcal/mol. In line with experimental observations, the formation of **6a** is kinetically favored over ***trans*-7a** and ***cis*-7a**. Coordination of the π-allyl fragment to Au(III) directs nucleophilic addition to the normally less reactive central position and drives the reaction to the formation of a metallacyclobutane instead of a π-olefin complex. This is in agreement with the MO analysis described above, with significant contributions of the central carbon atom of the π-allyl in the LUMO+2 of the gold complex **2**, which is accessible in energy and close to the LUMO and LUMO+1. In line with experimental observations, the auracyclobutane **6a** can reconvert into the π-allyl complex **2** and diethyl malonate **3a** ($\Delta G^{\neq}$ 27.0 kcal/mol for the reverse process). The reversibility of the nucleophilic attack at C_{cent} opens the way to the formation of the more stable π-alkene Au(I) complexes. Yet, ***trans*-7a** and ***cis*-7a** are not observed experimentally because they spontaneously evolve into the allylation product **4a** and (P,C)-cyclometallated gold(I) dimer **5** (the latter process was predicted to be further downhill in energy by 6.6 kcal/mol from ***trans*-7a**, see Table S4).[12] The direct formation of π-alkene complexes ***trans*-7a** and ***cis*-7a** from auracyclobutane **6a** (through ring-opening and 1,2-migration of the malonate) has also been envisioned as an alternative to the reversible attack of **3a** at C_{cent}, but the corresponding activation barriers are prohibitively high ($\Delta G^{\neq}$ > 100 kcal/mol).

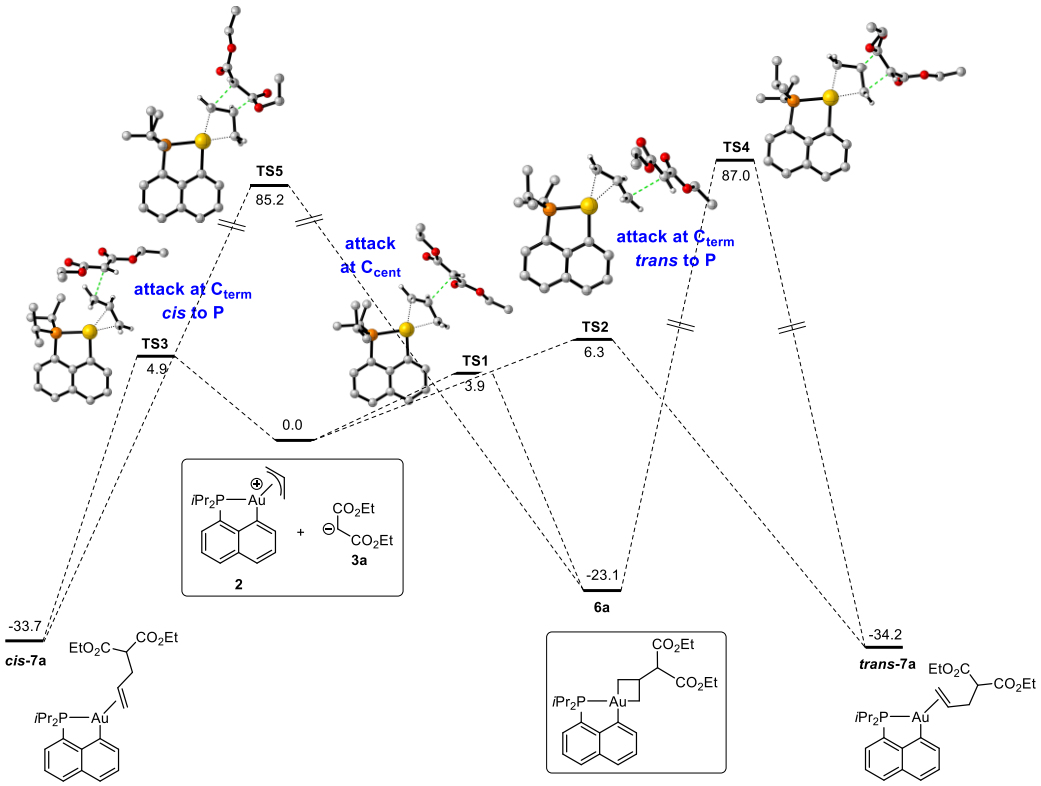


Figure 8. Energy profiles for the nucleophilic addition of enolate **3a** to the π-allyl Au(III) complex **2** computed at the SMD(THF)-B3PW91/SDD+f(Au),6-31G**(other atoms) level of theory. Gibbs free energies (ΔG) in kcal/mol.

Then, the Activation Strain Model (ASM) approach[20] was used to assess the relative contributions of the strain and interaction terms, and compare the nucleophilic attack of **3a** at the central / terminal positions of the π-allyl complex **2**. The corresponding diagrams for the two most favorable paths, *ie* the reactions at C_{cent} (**TS1**) and C_{term} *cis* to P (**TS3**) are displayed in Figure 9 (see Figure S67 for complete data).[12] Accordingly, the strain energy ΔE_{strain} is smaller for the attack at C_{cent} than at C_{term} along the entire reaction coordination ζ (C···C distance of the forming bond between the β-diketo enolate and the π-allyl). Moreover, the difference between the two increases as the reaction proceeds and approaches the transition state region. Comparatively, the interaction energy term ΔE_{int} for the attacks at C_{cent} than at C_{term} remains close. It is slightly larger for the addition to C_{cent} in the early stage of the reaction (till ~ 2.8 Å) and then reverses to become slightly larger for the addition to C_{term}. At a C···C distance of about 2.74 Å, near the transition states, the difference in the ΔE_{int} term is of only 0.8 kcal/mol in favor of the addition to C_{term}, while the ΔE_{strain} term for attack at C_{term} exceeds that at C_{cent} by 2.1 kcal/mol (Table S9).[12] Decomposition of this ΔE_{strain} term over the two fragments reveals it is primarily due to the deformation of the (P,C)Au(π-allyl)$^+$ complex. Analysis of the geometric changes on the paths to **TS1** and **TS3** shows that the largest difference arises from the allyl moiety. Upon attack at C_{cent} (**TS1**), the allyl group remains symmetrically η^3-coordinated to gold. In contrast, attack at C_{term} *cis* to P (**TS3**) induces some shift of the allyl group to η^1-coordination, which raises the distortion energy (Figures S68-69).[12]

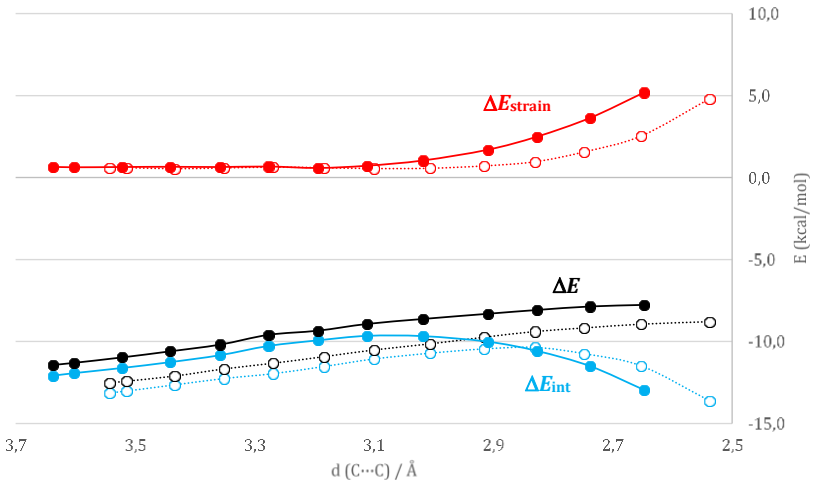


Figure 9. Comparison of the Activation Strain diagrams accounting for the nucleophilic attack of **3a** at C_{cent} (dotted lines) and C_{term} *cis* to P (solid lines) of the π-allyl complex **2** computed at SMD(THF)-B3PW91/SDD+f(Au),6-31G**(other atoms) level of theory.

Given the significant contribution of gold in the vacant orbitals of complex **2** (LUMO, LUMO+1 and LUMO+2) and the experimental characterization of the σ-allyl Au(III) complex **8'a** in the reaction **2'** + **3a**, the inner-sphere route to C–C coupling at Au(III) was also considered for the reaction **2** + **3a** (Figure 10). Shifting the allyl group from π (η^3) to σ (η^1) coordination to open a vacant site at gold is energetically demanding (~18 kcal/mol, Figure S62).[12] Nonetheless, direct attack of **3a** at the gold center of the π-allyl complex **2** turned to be quite easy, with activation barriers $\Delta G^{\neq}$ of 7.0 to 9.0 kcal/mol (for **TS7** and **TS8**, displacement of the Au–C(allyl) bond *cis* and *trans* to P, respectively). It is thermodynamically favored (ΔG –14.4 to –16.1 kcal/mol), but the ensuing σ-allyl Au(III) complexes ***trans*-8a** and ***cis*-8a** are higher in energy than the auracyclobutane **6a** by 7–9 kcal/mol. Nucleophilic attack at gold is thus neither kinetically nor thermodynamically favored over attack at C_{cent}. In any way, reductive elimination from ***trans*-8a** and ***cis*-8a** involves large activation barriers ($\Delta G^{\neq}$ > 50 kcal/mol), as expected for $C(sp^3)$–$C(sp^3)$ couplings from tetracoordinate Au(III) complexes.[21] If direct attack at gold is feasible, it is unproductive and the inner-sphere process cannot account for the formation of the allylation products. It is worth noting however that the formation of σ-allyl Au(III) complexes may be reversible, as that of the auracycle ($\Delta G^{\neq}$ 23–24 kcal/mol for the backward process from ***trans*-8a** and ***cis*-8a**), in line with that observed in the reaction **2'** + **3a**.

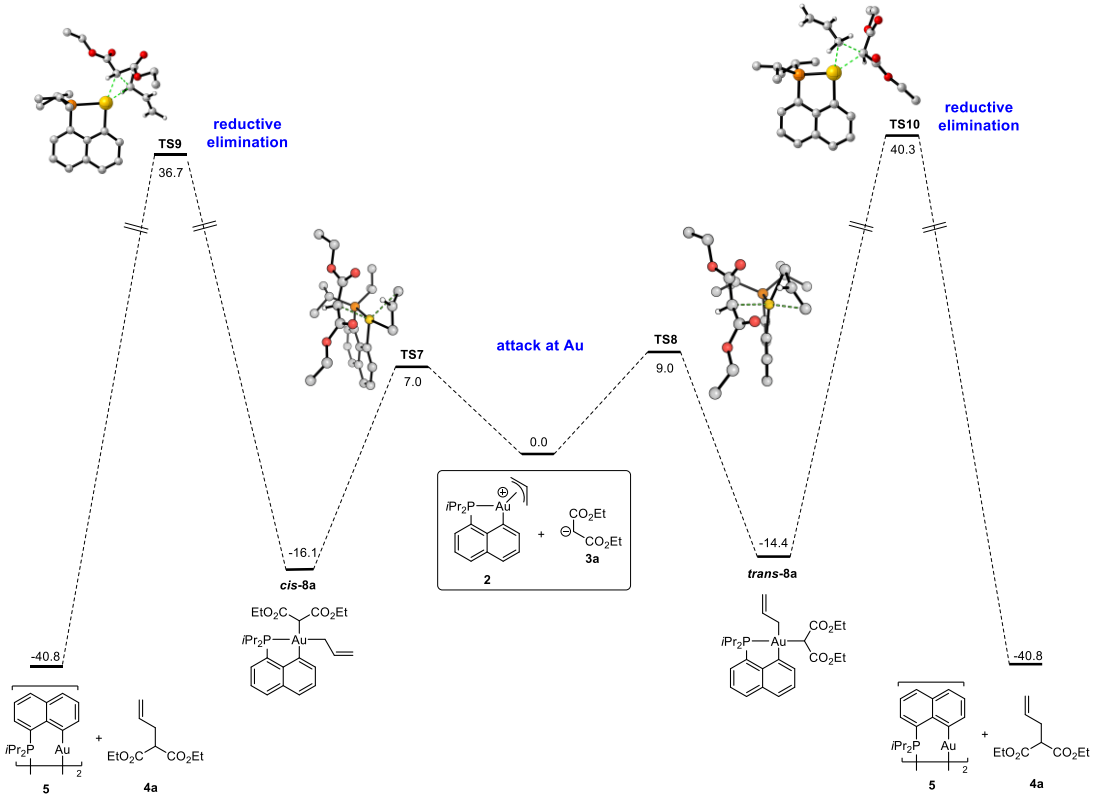


Figure 10. Alternative inner-sphere pathway for the reaction of enolate **3a** with the π-allyl Au(III) complex **2** computed at SMD(THF)-B3PW91/SDD+f(Au),6-31G**(other atoms) level of theory. Gibbs free energies (ΔG) in kcal/mol.

Energy profile for the reaction 2' + 3b

In the case of the reaction **2'** + **3b**, the π-alkene complex **7'b**, not the auracycle **6'b** was observed upon reaction monitoring. To gain more insight into the different regioselectivity of the two reactions, the nucleophilic attacks of β-diketo enolate **3b** to the central and terminal positions of the methallyl complex **2'** were computed (Figure 11). As expected, the methyl substituent makes addition to the central position more difficult. The formation of the auracyclobutane **6'b** from **2'** + **3b** is only slightly downhill in energy (ΔG –5.3 kcal/mol) and the associated activation barrier $\Delta G^{\neq}$ amounts to 12.9 kcal/mol. Because of the formation of a quaternary C atom, this barrier is about 9 kcal/mol higher than that computed for the reaction **2** + **3a** and the formation of the auracycle **6'b** is less favorable thermodynamically than that of **6a** by 18 kcal/mol. Moreover, and in contrast to what was observed for the reaction **2** + **3a**, the nucleophilic attack of **3b** at the central position of **2'** is less favorable kinetically and thermodynamically than at the terminal carbon atoms (*cis* to P, $\Delta G^{\neq}$ 9.5 kcal/mol, ΔG –16.6 kcal/mol, and *trans* to P, $\Delta G^{\neq}$ 12.1 kcal/mol, ΔG –17.6 kcal/mol). Of note, the activation barrier for the nucleophilic attack *trans* to C is 2.5 kcal/mol lower than that *trans* to P, as expected from the stronger σ-donor character and *trans* effect of C over P.[14] In line with experimental observations, the resulting π-alkene complexes ***cis*-** and ***trans*-7'b** are close in energy (ΔG 1.0 kcal/mol) and were predicted to easily interconvert by rotation of the C=C bond with respect to the (P,C)Au coordination plane (the corresponding transition state $\mathbf{TS_{isom}}$ lies <10 kcal/mol higher in energy).[22] The most stable π-complex ***trans*-7'b** is the one with the CH_2 end of the alkene *cis* to P. This nicely matches with ***trans*-7'b-Cy** found as the major form in solution by low temperature NMR spectroscopy and crystallographic characterization. Evolution of the π-alkene complexes **7'b** over time to release the free olefin **4'b** and the (P,C)-cyclometallated Au(I) dimer **5** is further downhill in energy (by 10.1 kcal/mol from ***trans*-7'b**, Table S4).[12]

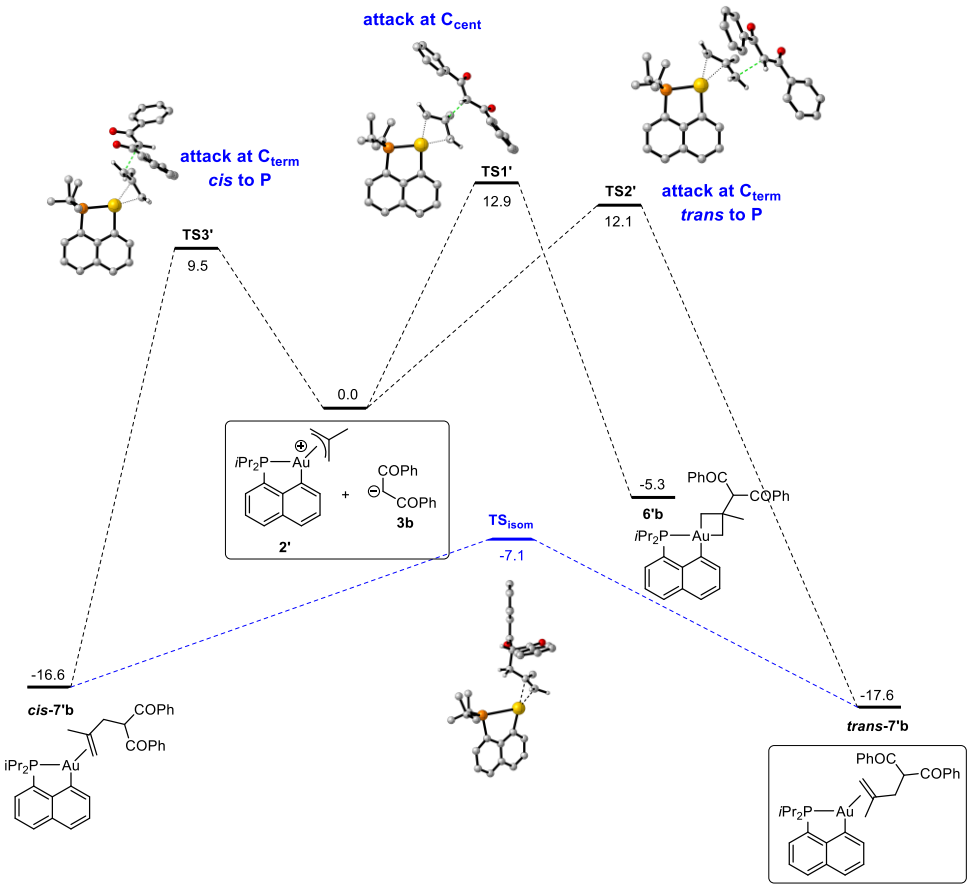


Figure 11. Energy profiles for the nucleophilic addition of enolate **3b** to the π-methallyl Au(III) complex **2'** computed at the SMD(THF)-B3PW91/SDD+f(Au),6-31G**(other atoms) level of theory. Gibbs free energies (ΔG) in kcal/mol.

The activation strain diagrams for the reaction **2'** + **3b** are depicted in Figure 12 (see Figure S72 for complete data).[12] Compared to the reaction **2** + **3a**, the additional methyl substituent on the allyl increases the deformation cost. The strain energy term ΔE_{strain} is again smaller for the attack at C_{cent} than at C_{term} but the difference between the two is less than for the reaction **2** + **3a**. The energy term ΔE_{int} is more stabilizing for the nucleophilic addition to C_{term} along the entire reaction coordinate for **2'** + **3b.** The methyl group somewhat shields the nucleophilic attack at C_{cent} that leads to the formation a quaternary C atom. Accordingly, the difference between the terminal/central sites of the π-allyl stems primarily from the interaction energy term ΔE_{int} in this case: at a C···C distance of about 2.45 Å, it favors attack at C_{term} by 4.4 kcal/mol while the strain energy term ΔE_{strain} is 3.4 kcal/mol larger (Table S11).[12] According to Energy Decomposition Analysis, the main stabilizing contribution to the ΔE_{int} term comes from the electrostatic term (ΔE_{elstat}) which accounts for ~ 70 % of the total attractive interaction energy in both cases (Table S12).[12] The largest difference between the attacks at C_{term} and C_{cent} is found in the orbital term (ΔE_{orb}). It is more stabilizing for C_{term} (ΔE_{orb} –36.9 kcal/mol) than for C_{cent} (–32.4 kcal/mol). The Natural Orbital for Chemical Valence (NOCV) extension of the EDA method indicates that the orbital interaction is primarily due to the donation from the π orbital of β-enolate fragment (delocalized over the 3 carbon atoms) to the terminal/central positions of the (P,C)Au(methallyl)$^+$ moiety (Figure S73).[12]

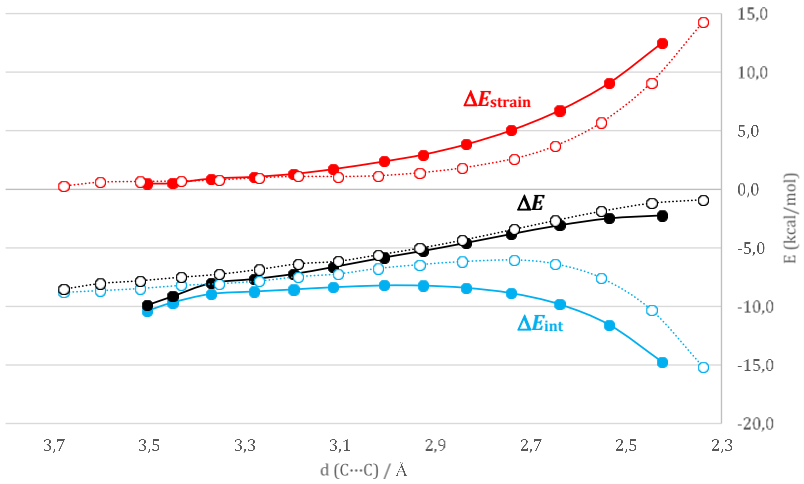


Figure 12. Comparison of the Activation Strain diagrams accounting for the nucleophilic attack of **3b** at C_{cent} (dotted lines) and C_{term} *cis* to P (solid lines) of the π-methallyl complex **2'** computed at SMD(THF)-B3PW91/SDD+f(Au),6-31G**(other atoms) level of theory.

The energy profiles computed for the reactions **2** + **3a** and **2'** + **3b** are in good agreement with the NMR monitoring and the experimental characterization of the auracyclobutane **6a** and π-alkene complex **7'b**. They confirm that nucleophilic attack at the terminal and central positions of the allyl (as well as gold itself) are all possible and actually competitive. As a result, the favored regioselectivity depends subtly on the combination of π-allyl Au(III) complex and β-diketo enolate. The formation of metallacyclobutanes is more favorable for Au(III) than for Pd(II) complexes, and thus intrinsically competitive with the formation π-alkene complexes in the case of gold. Nucleophilic attack at the central position of the allyl is less favored when it is substituted (as in the reaction **2'** + **3b**), but it remains feasible, as observed in the reaction of the methallyl complex **2'** with diethyl malonate **3a**.

Taking into account that **7'b** is the first example of a cyclometallated Au(I) π-complex, its structure was thoroughly analyzed and compared with that of other gold(I) π-complexes, in particular 3-coordinate species.[7e] For sake of simplicity, only ***trans*-7'b** is discussed here but ***cis*-7'b** was also considered and the bonding situation was found to be very similar in both forms (Table S5).[12] The optimized geometry of ***trans*-7'b** nicely reproduces the X-ray diffraction structure of ***trans*-7'b-Cy** (Table S5).[12] The alkene is in-plane side-on coordinated to gold, with noticeable elongation of the C=C double bond (1.432 Å) compared to the free olefin **4'b** (1.339 Å). The presence of significant Au→π*(C=C) backdonation in **7'b** is clearly apparent from Charge Decomposition Analysis (CDA). The donation/back-donation ratio d/b (1.65) falls in the lower range of those reported for gold(I) π-complexes. It is actually similar to that found with the (P,N)-chelating ligand MeDalphos and methacrylate, an electron-poor alkene (d/b 1.77).[23] A strong d(Au)→π*(C=C) donor-acceptor interaction (stabilizing interaction ΔE 45.1 kcal/mol) is also found by Natural Bond Orbital (NBO) analysis (Figure 13). Consistently, the C=C bond is noticeably weakened, as shown from the Wiberg bond index (1.348 in ***trans*-7'b** *versus* 1.916 for the free alkene **4'b**). Comparing ***trans*-7'b** with the isomerization transition state $\mathbf{TS_{isom}}$ is also relevant and informative (Tables S5-S6 and Figure S66).[12] In the latter case, the alkene is about perpendicular to the (P,C)Au coordination plane, minimizing Au→π*(C=C) back-donation. As a result, the C=C distance (1.379 Å) and ΔE[Au→π*(C=C)] (25.1 kcal/mol) are significantly lower, while the Wiberg bond index is higher (1.616). Finally, it is worth noting that the strong Au→π*(C=C) backdonation and metallacyclopropane character of **7'b** are consistent with the significant upfield shift of the ^{1}H and ^{13}C alkene resonances (Table S7).[12]

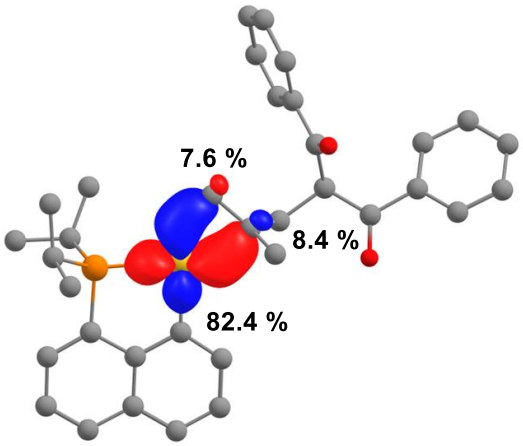
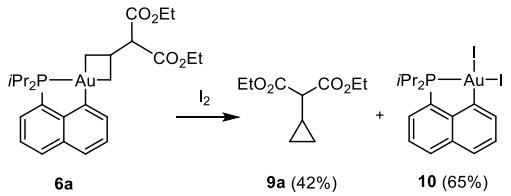


Figure 13. NLMO associated to d(Au)→π*(C=C) back-donation in the (P,C)-cyclometallated Au(I) π-complex ***trans*-7'b**, with participation of main atoms in % (cutoff: 0.05). Hydrogen atoms have been omitted for clarity.

Part III. Auracyclobutanes, relevant intermediates in cyclopropanation reactions at gold

On the basis of computational studies, auracyclobutanes have been evoked as possible intermediates in gold-mediated cyclopropanation of alkenes,[24] but no experimental evidence for such a process has been reported so far. Having access to auracyclobutanes by nucleophilic addition to the central position of π-allyl Au(III) complexes, we sought to probe their faculty to form the corresponding cyclopropanes. To this end, the auracyclobutane **6a** was reacted with an excess of I_2 (Scheme 7)[25] right after its formation from **2** + **3a**. Pleasingly, C–C coupling occurred before **6a** rearranged to release the C-allylation product **4a**. Instead, the desired cyclopropane **9a** was obtained, along with the P,C-cyclometallated Au(III) diiodo complex **10**.[26] Thus, auracyclobutanes can readily afford cyclopropanes despite the strain of the 3-membered ring and the low tendency of Au(III) complexes to undergo C(sp^3)–C(sp^3) coupling.[21]



Scheme 7. Oxidative C–C coupling of the auracyclobutane **6a** leading to cyclopropane **9a** along with the P,C-cyclometallated Au(III) diiodo complex **10**.

Conclusion

In summary, with Au(III) π-allyl complexes, nucleophilic additions to the central and terminal positions as well as gold are all possible and are intrinsically competitive. This is in contrast with the well-documented Pd(II) π-allyl complexes where addition to the terminal carbon atoms prevails. Meticulous low temperature NMR monitoring of reactions between Au(III) π-allyl complexes **2/2'** and β-diketo enolates **3a-c** enabled to characterize auracyclobutanes **6**, π-alkene Au(I) complexes **7** as well as σ-allyl Au(III) complexes **8**. All reactions lead ultimately to the formation of the C-allylation product **4** along with the (P,C)-cyclometallated Au(I) dimer **5**. Nucleophilic attacks at the central position and at gold are reversible.

Detailed analysis of the electronic properties of the π-allyl gold(III) complexes, combined with the reaction profiles for the nucleophilic attacks at C_{term}, C_{cent} and Au provide valuable insight into the intrinsic

competition between the reactive sites, the key factors at play, and highlight the differences between Au(III) and Pd(II) π-allyl complexes.

The auracyclobutane **6a** and Au(I) π-alkene complex **7'b** have been isolated and fully characterized (including by X-ray diffraction for their PCy_2 analogues). Treatment of **6a** with iodine induced $C(sp^3)$–$C(sp^3)$ coupling and afforded the corresponding cyclopropane **9a**, demonstrating the relevance of auracyclobutanes in gold-mediated cyclopropanation reaction and cyclopropane ring-opening. Complex **7'b** is the first gold(I) π-complex featuring a cyclometallated ligand to be reported. Backdonation, for which gold is usually lazy, is significant, as apparent from its spectroscopic and structural data, as well as theoretical analysis of its bonding situation.

Detailed understanding of the reactivity of Au(III) π-allyl complexes is of fundamental and synthetic interest. This first study points out the possible involvement and competition between the different reactive sites of the Au(III) π-allyl complexes, and at the same time the reversibility of the nucleophilic additions at the central position and gold, so that the allylated product originating from the attack at the terminal position is ultimately obtained in all cases. Next steps are *i*) to determine how general is this picture in terms of nucleophiles (C-, N- and O-based, soft *versus* hard nucleophiles), allyl group (alkyl/aryl-substituted at the central/terminal positions) and ancillary ligand at gold (P,C- *versus* N,C-cyclometallated species depicted in Figure 2), *ii*) to understand what influences the efficiency of the allylation reaction (in terms of yield and rate) and its selectivity when dealing with unsymmetrical π-allyl (linear *versus* branched products)? and *iii*) to further outline the common and different features of Au(III) and Pd(II) π-allyl complexes. More studies are also needed to identify the conditions of formation and stability of auracyclobutanes, as well as to explore further their reactivity. Finally, developing catalytic allylation reactions involving Au (III) π-allyl complexes is also highly attractive.[27] To this end, one may take advantage of the approaches recently developed to cycle between Au(I) and Au(III) oxidation states and perform 2-electron redox catalysis.[28]

SUPPORTING INFORMATION

The Supporting Information is available free of charge at htttps//pubs.acs.org/doi/.

Experimental and computational details, analytical data and NMR spectra (PDF)

Optimized cartesian coordinates (XYZ)

CCDC-2079647 (**5-Cy**), 2079648 (**6c-Cy**) and 2079649 (***trans*-7'b-Cy**) contain the supplementary crystallographic data for this paper. These data can be obtained free of charge via www.ccdc.cam.ac.uk/data_request/cif, or by emailing data_request@ccdc.cam.ac.uk, or by contacting The Cambridge Crystallographic Data Centre, 12 Union Road, Cambridge CB2 1EZ, UK; fax: + 44 1223 336033.

ACKNOWLEDGMENTS

This article is dedicated to Odile Eisenstein. The Centre National de la Recherche Scientifique (CNRS), the Université Paul Sabatier (UPS) and the Agence Nationale de la Recherche (ANR-19-CE07-0037) are gratefully acknowledged for financial support of this work. J. R. thanks the European Commission for a MCIF (Gold3Cat-799606). The "Direction du Numérique" of the Université de Pau et des Pays de l'Adour, CINES under allocation A009080045 made by Grand Equipement National de Calcul Intensif (GENCI) and Mésocentre de Calcul Intensif Aquitain (MCIA) are acknowledged for computational facilities.

AUTHORS

Jessica Rodriguez, Marte Sofie Martinsen Holmsen, Didier Bourissou*: CNRS/Université de Toulouse, UPS, Laboratoire Hétérochimie Fondamentale et Appliquée – LHFA UMR 5069, 118 route de Narbonne, 31062 Toulouse, France.*

Yago García-Rodeja, E. Daiann Sosa Carrizo, Karinne Miqueu: *CNRS/Université de Pau et des Pays de l'Adour, E2S-UPPA, Institut des Sciences Analytiques et de Physico-Chimie pour l'Environnement et les Matériaux - IPREM UMR 5254. Hélioparc, 2 Avenue du Président Angot, 64053 Pau Cedex 09, France.*

Pierre Lavedan, Sonia Mallet-Ladeira: *CNRS/Université de Toulouse, UPS, Institut de Chimie de Toulouse – ICT, 118 Route de Narbonne, 31062 Toulouse Cedex 09, France.*

REFERENCES

(1) (a) Trost, B. M.; Crawley, M. L. Asymmetric Transition-Metal-Catalyzed Allylic Alkylations: Applications in Total Synthesis. *Chem. Rev.* **2003**, *103*, 2921–2944; (b) Pàmies, O.; Margalef, J.; Cañellas, S.; James, J.; Judge, E.; Guiry, P. J.; Moberg, C.; Bäckvall, J.-E.; Pfaltz, A.; Pericàs, M. A.; Diéguez, M. Recent Advances in Enantioselective Pd-Catalyzed Allylic Substitution: From Design to Applications. *Chem. Rev.* **2021**, https://doi.org/10.1021/acs.chemrev.0c00736.

(2) Hartwig, J. F. *Organotransition Metal Chemistry: From Bonding to Catalysis*. University Science Books, Sausalito, 2010, 1160 pp.

(3) (a) Keith, J. A.; Behenna, D. C.; Sherden, N.; Mohr, J. T.; Ma, S.; Marinescu, S. C.; Nielsen, R. J.; Oxgaard, J.; Stoltz, B. M.; Goddard, W. A. The Reaction Mechanism of the Enantioselective Tsuji Allylation: Inner-Sphere and Outer-Sphere Pathways, Internal Rearrangements, and Asymmetric C–C Bond Formation. *J. Am. Chem. Soc.* **2012**, *134*, 19050–19060; (b) Cusumano, A. Q.; Stoltz, B. M.; Goddard, W. A. Reaction Mechanism, Origins of Enantioselectivity, and Reactivity Trends in Asymmetric Allylic Alkylation: A Comprehensive Quantum Mechanics Investigation of a $C(sp^3)$−$C(sp^3)$ Cross-Coupling. *J. Am. Chem. Soc.* **2020**, *142*, 13917–13933; (c) Ardolino, M. J.; Morken, J. P. Congested C–C Bonds by Pd-Catalyzed Enantioselective Allyl–Allyl Cross-Coupling, a Mechanism-Guided Solution. *J. Am. Chem. Soc.* **2014**, *136*, 7092–7100; (d) Bai, D.-C.; Yu, F.-L.; Wang, W.-Y.; Chen, D.; Li, H.; Liu, Q.-R.; Ding, C.-H.; Chen, B.; Hou, X.-L. Palladium/*N*-heterocyclic carbene catalysed regio and diastereoselective reaction of ketones with allyl reagents via inner-sphere mechanism. *Nature Commun.* **2016**, *7*, 11806; (e) Hu, L.; Cai, A.; Wu, Z.; Kleij, A. W.; Huang, G. A Mechanistic Analysis of the Palladium-Catalyzed Formation of Branched Allylic Amines Reveals the Origin of the Regio- and Enantioselectivity through a Unique Inner-Sphere Pathway. *Angew. Chem. Int. Ed.* **2019**, *58*, 14694–14702 and references therein.

(4) (a) Ephritikhine, M.; Francis, B. R.; Green, M. L. H.; Mackenzie, R. E.; Smith, M. J. Bis(η-cyclopentadienyl)-molybdenum and -tungsten chemistry: σ- and η-allylic and metallacyclobutane derivatives. *J. Chem. Soc. Dalton Trans.* **1977**, 1131–1135; (b) Ephritikhine, M.; Green, M. L. H.; MacKenzie, R. E. Some η^1 and η^3-allylic and metallocyclobutane derivatives of molybdenum and tungsten. *J. Chem. Soc., Chem. Commun.* **1976**, 619–621.

(5) (a) Periana, R. A.; Bergman, R. G. Rapid intramolecular rearrangement of a hydrido(cyclopropyl)rhodium complex to a rhodacyclobutane. Independent synthesis of the metallacycle by addition of hydride to the central carbon atom of a cationic rhodium π-allyl complex. *J. Am. Chem. Soc.* **1984**, *106*, 7272–7273; (b) McGhee, W. D.; Bergman, R. G. Synthesis and reactions of hydrido(η^1-allyl)- and hydrido(η^3-allyl)iridium complexes. *J. Am. Chem. Soc.* **1985**, *107*, 3388–3389; (c) Tjaden, E. B.; Stryker, J. M. Nucleophilic addition of enolates to the central carbon of transition-metal η^3-allyl complexes. Metallacyclobutane formation, reversibility of nucleophilic addition, and synthesis of .alpha.-cyclopropyl ketones. *J. Am. Chem. Soc.* **1990**, *112*, 6420–6422; (d) Wakefield, J. B.; Stryker, J. M. Metallacyclobutanes from kinetic nucleophilic addition to η^3-allyl ethylene complexes of iridium. Regioselectivity dependence on nucleophile and allyl orientation. *J. Am. Chem. Soc.* **1991**, *113*, 7057–7059; (e) Tjaden, E. B.; Schwiebert, K. E.; Stryker, J. M. Strong organometallic anomeric effects. Long-range stereoelectronic control of cyclohexanone conformation via a transannular metallacyclobutane interaction. *J. Am. Chem. Soc.* **1992**, *114*, 1100–1102; (f) Tjaden, E. B.; Stryker, J. M. Metallacyclobutanes from (η^3-crotyl)rhodium complexes: regioselectivity dependence on allyl ligand configuration. Reinvestigation of nucleophilic additions to two isomers of [CpRh(*iso*-Pr_3P)(η^3-crotyl)]BF_4. *Organometallics* **1992**, *11*, 16–18; (g) For reactions of a π-allyl Ir(III) complex featuring a chiral (P,N) ligand with a malonate, see: García-Yebra, C.; Janssen, J. P.; Rominger, F.; Helmchen, G. Asymmetric Iridium(I)-Catalyzed Allylic Alkylation of Monosubstituted Allylic Substrates with Phosphinooxazolines as Ligands. Isolation, Characterization, and Reactivity of Chiral (Allyl)iridium(III) Complexes. *Organometallics* **2004**, *23*, 5459–5470.

(6) (a) Hoffmann, H. M. R.; Otte, A. R.; Wilde, A. Nucleophilic Attack at the Central Carbon Atom of (π-Allyl)palladium Complexes: Formation of α-Cyclopropyl Esters. *Angew. Chem. Int. Ed.* **1992**, *31*, 234–

236; (b) Wilde, A.; Otte, A. R.; Hoffmann, H. M. R. Cyclopropanes via nucleophilic attack at the central carbon of (π-allyl)palladium complexes. *J. Chem. Soc., Chem. Commun.* **1993**, 615–616; (c) Otte, A. R.; Wilde, A.; Hoffmann, H. M. R. Cyclopropanes by Nucleophilic Attack of Mono-and Diaryl-Substituted (η^3-Allyl)palladium Complexes: Aryl Effect and Stereochemistry. *Angew. Chem. Int. Ed.* **1994**, *33*, 1280–1282; (d) Hoffmann, H. M. R.; Otte, A. R.; Wilde, A.; Menzer, S.; Williams, D. J. Isolation and X-Ray Crystal Structure of a Palladacyclobutane: Insight into the Mechanism of Cyclopropanation. *Angew. Chem. Int. Ed.* **1995**, *34*, 100–102; (e) Shintani, R.; Tsuji, T.; Park, S.; Hayashi, T. Mechanistic Investigation of the Palladium-Catalyzed Decarboxylative Cyclization of γ-Methylidene-δ-valerolactones with Isocyanates: Kinetic Studies and Origin of the Site Selectivity in the Nucleophilic Attack at a (π-Allyl)palladium. *J. Am. Chem. Soc.* **2010**, *132*, 7508–7513; (f) Shintani, R.; Moriya, K.; Hayashi, T. Guiding the nitrogen nucleophile to the middle: palladium-catalyzed decarboxylative cyclopropanation of 2-alkylidenetrimethylene carbonates with isocyanates. *Chem. Commun.* **2011**, *47*, 3057–3059.

(7) (a) Schmidbaur, H.; Schier, A. Gold η^2-Coordination to Unsaturated and Aromatic Hydrocarbons: The Key Step in Gold-Catalyzed Organic Transformations. *Organometallics* **2010**, *29*, 2–23; (b) Brooner, R. E. M.; Widenhoefer, R. A. Cationic, Two-Coordinate Gold π-Complexes. *Angew. Chem. Int. Ed.* **2013**, *52*, 11714–11724; (c) Blons, C.; Amgoune, A.; Bourissou, D. Gold(III) π complexes. *Dalton Trans.* **2018**, *47*, 10388–10393; (d) Herrera, R. P.; Gimeno, M. C. Main Avenues in Gold Coordination Chemistry. *Chem. Rev.* **2021**, https://dx.doi.org/10.1021/acs.chemrev.0c00930; (e) Navarro, M.; Bourissou, D. π-Alkene/alkyne and carbene complexes of gold(I) stabilized by chelating ligands, *Adv. Organomet. Chem.* **2021**, *76*, 101–144.

(8) Holmsen, M. S. M.; Nova, A.; Øien-Ødegaard, S.; Heyn, R. H.; Tilset, M. A Highly Asymmetric Gold(III) η^3-Allyl Complex. *Angew. Chem. Int. Ed.* **2020**, *59*, 1516–1520.

(9) Rodriguez, J.; Szalóki, G.; Sosa Carrizo, E. D.; Saffon-Merceron, N.; Miqueu, K.; Bourissou, D. Gold(III) π-Allyl Complexes. *Angew. Chem. Int. Ed.* **2020**, *59*, 1511–1515.

(10) For σ-allyl Au(III) complexes, see: (a) Sanshiro, K.; Satoshi, O. Isolation of the First Allylic Gold(III) Complex Having a Triphenylphosphine Ligand. *Chem. Lett.* **1988**, *17*, 1431–1432; (b) Levin, M. D.; Toste, F. D. Gold-Catalyzed Allylation of Aryl Boronic Acids: Accessing Cross-Coupling Reactivity with Gold. *Angew. Chem. Int. Ed.* **2014**, *53*, 6211–6215; (c) Levin, M. D.; Chen, T. Q.; Neubig, M. E.; Hong, C. M.; Theulier, C. A.; Kobylianskii, I. J.; Janabi, M.; O'Neil, J. P.; Toste, F. D. A catalytic fluoride-rebound mechanism for $C(sp^3)$–CF_3 bond formation. *Science* **2017**, *356*, 1272–1276; (d) For σ-allenyl Au(I/III) complexes, see: Johnson, A.; Laguna, A.; Concepción Gimeno, M. Axially Chiral Allenyl Gold Complexes. *J. Am. Chem. Soc.* **2014**, *136*, 12812–12815; (e) For 1,1-digold(I) allylium complexes, see: Mulks, F. F.; Antoni, P. W.; Gross, J. H.; Graf, J.; Rominger, F.; Hashmi, A. S. K. 1,1-Digoldallylium Complexes: Diaurated Allylic Carbocations Indicate New Prospects of the Coordination Chemistry of Carbon. *J. Am. Chem. Soc.* **2019**, *141*, 4687–4695.

(11) The NMR data of a few Ir, Rh and Pt metallacyclobutanes have been assigned in detail, showing similar shielding. See ref 5a,c and Carfagna, C.; Galarini, R.; Musco, A.; Santi, R. Platinacyclobutane complexes from nucleophilic attack at a coordinated allyl group and catalytic formation of cyclopropanes in the presence of platinum complexes. *Organometallics* **1991**, *10*, 3956–3958.

(12) See supporting information for details.

(13) Dinger, M. B.; Henderson, W. Synthesis and characterization of the first auracyclobutane complex. *J. Organomet. Chem.* **1999**, *577*, 219–222.

(14) (a) Langseth, E.; Nova, A.; Tråseth, E. A.; Rise, F.; Øien, S.; Heyn, R. H.; Tilset, M. A Gold Exchange: A Mechanistic Study of a Reversible, Formal Ethylene Insertion into a Gold(III)–Oxygen Bond. *J. Am. Chem. Soc.* **2014**, *136*, 10104–10115; (b) Holmsen, M. S. M.; Nova, A.; Balcells, D.; Langseth, E.; Øien-Ødegaard, S.; Heyn, R. H.; Tilset, M.; Laurenczy, G. *trans*-Mutation at Gold(III): A Mechanistic Study of a Catalytic Acetylene Functionalization via a Double Insertion Pathway. *ACS Catal.* **2017**, *7*, 5023–5034.

(15) Curtis, M. D.; Eisenstein, O. A molecular orbital analysis of the regioselectivity of nucleophilic addition to .eta.3-allyl complexes and the conformation of the η^3-allyl ligand in $L_3(CO)_2(\eta^3\text{-}C_3H_5)Mo(II)$ complexes. *Organometallics* **1984**, *3*, 887–895.

(16) Carfagna, C.; Galarini, R.; Linn, K.; Lopez, J. A.; Mealli, C.; Musco, A. Nucleophilic attack at the central allyl carbon atom in $[(\eta^3\text{-allyl})ML_2]^+$ complexes (M = palladium, platinum). Experimental facts and new theoretical insights. *Organometallics* **1993**, *12*, 3019–3028.

(17) For a perspective dealing with computational studies of C–C bond formation involving allyl palladium complexes, see: Cárdenas, D. J.; Echavarren, A. M. Mechanistic aspects of C–C bond formation involving allylpalladium complexes: the role of computational studies. *New J. Chem.* **2004**, *28*, 338–347.

(18) (a) Gorelsky, S. I. *AOMix: Program for Molecular Orbital Analysis*, http://www.sg-chem.net, version 6.94, 2019; (b) Gorelsky, S. I.; Lever, A. B. P. Electronic structure and spectra of ruthenium diimine complexes by density functional theory and INDO/S. Comparison of the two methods. *J. Organomet. Chem.* **2001**, *635*, 187–196.
(19) The bonding interaction of π3 with the lumo of (P,C)Au leads to another vacant orbital, LUMO+4 (Figure S53).[12] It is found at –0.33 eV, about 1 eV above LUMO+2, with again main contributions from Ccent (19.9%) and Au (14.5%).
(20) For recent reviews, see: (a) Fernández, I.; Bickelhaupt, F. M. The activation strain model and molecular orbital theory: understanding and designing chemical reactions. *Chem. Soc. Rev.* **2014**, *43*, 4953–4967; (b) Wolters, L. P.; Bickelhaupt, F. M. The activation strain model and molecular orbital theory. *WIREs Comput. Mol. Sci.* **2015**, *5*, 324–343; (c) Bickelhaupt, F. M.; Houk, K. N. Analyzing Reaction Rates with the Distortion/Interaction-Activation Strain Model. *Angew. Chem. Int. Ed.* **2017**, *56*, 10070–10086; (d) Vermeeren, P.; van der Lubbe, S. C. C.; Fonseca Guerra, C.; Bickelhaupt, F. M.; Hamlin, T. A. Understanding chemical reactivity using the activation strain model. *Nat. Protoc.* **2020**, *15*, 649–667; (e) Férnandez, I., Discovering the Future of Molecular Sciences. Pignataro, B., Ed. Wiley-VCH, Weinheim, **2014**, pp 165–187.
(21) For selected references, see: (a) Kaphan, D. M.; Levin, M. D.; Bergman, R. G.; Raymond, K. N.; Toste, F. D. A supramolecular microenvironment strategy for transition metal catalysis. *Science* **2015**, *350*, 1235–1238; (b) Nijamudheen, A.; Karmakar, S.; Datta, A. Understanding the Mechanisms of Unusually Fast H–H, C–H, and C–C Bond Reductive Eliminations from Gold(III) Complexes. *Chem. Eur. J.* **2014**, *20*, 14650–14658; (c) Norjmaa, G.; Maréchal, J.-D.; Ujaque, G. Microsolvation and Encapsulation Effects on Supramolecular Catalysis: C–C Reductive Elimination inside $[Ga_4L_6]^{12-}$ Metallocage. *J. Am. Chem. Soc.* **2019**, *141*, 13114–13123; (d) Welborn, V. V.; Li, W.-L.; Head-Gordon, T. Interplay of water and a supramolecular capsule for catalysis of reductive elimination reaction from gold. *Nat. Commun.* **2020**, *11*, 415.
(22) A dissociative pathway has also been considered for exchanging ***cis*-** and ***trans*-7'b**, but it is more demanding in energy ($\Delta G^{\neq} > 20$ kcal/mol, Figure S65).[12]
(23) Navarro, M.; Toledo, A.; Mallet-Ladeira, S.; Sosa Carrizo, E. D.; Miqueu, K.; Bourissou, D. Versatility and adaptative behaviour of the P^N chelating ligand MeDalphos within gold(I) π complexes. *Chem. Sci.* **2020**, *11*, 2750–2758.
(24) (a) Batiste, L.; Fedorov, A.; Chen, P. Gold carbenes via 1,2-dialkoxycyclopropane ring-opening: a mass spectrometric and DFT study of the reaction pathways. *Chem. Commun.* **2010**, *46*, 3899–3901; (b) Fedorov, A.; Batiste, L.; Bach, A.; Birney, D. M.; Chen, P. Potential Energy Surface for (Retro)Cyclopropanation: Metathesis with a Cationic Gold Complex. *J. Am. Chem. Soc.* **2011**, *133*, 12162–12171.
(25) For iodinolysis of Pt and Ir metallacyclobutanes leading to cyclopropanes, see ref 5c and Foley, P.; Whitesides, G. M. Thermal generation of bis(triethylphosphine)-3,3-dimethylplatinacyclobutane from dineopentylbis(triethylphosphine)platinum(II). *J. Am. Chem. Soc.* **1979**, *101*, 2732–2733.
(26) Rekhroukh, R.; Brousses, R.; Amgoune, A.; Bourissou D. Cationic Gold(III) Alkyl Complexes: Generation, Trapping, and Insertion of Norbornene. *Angew. Chem. Int. Ed.* **2015**, *54*, 1266–1269.
(27) Gold-catalyzed allylations are rare and none of them are supposed to involve π-allyl complexes: (a) Levin, M. D.; Toste, F. D. Gold‐Catalyzed Allylation of Aryl Boronic Acids: Accessing Cross-Coupling Reactivity with Gold. *Angew. Chem. Int. Ed.* **2014**, *53*, 6211–6215; (b) Akram, M. O.; Mali, P. S.; Patil, N. T. Cross-Coupling Reactions of Aryldiazonium Salts with Allylsilanes under Merged Gold/Visible-Light Photoredox Catalysis. *Org. Lett.* **2017**, *19*, 3075–3078; (c) Wang, J.; Zhang, S.; Xu, C.; Wojtas, L.; Akhmedov, N. G.; Chen, H.; Shi, X. Highly Efficient and Stereoselective Thioallylation of Alkynes: Possible Gold Redox Catalysis with No Need for a Strong Oxidant. *Angew. Chem. Int. Ed.*, **2018**, *57*, 6915–6920; (d) Holz, J.; Pfeffer, C.; Zuo, H.; Beierlein, D.; Richter, G.; Klemm, E.; Peters, R. In Situ Generated Gold Nanoparticles on Active Carbon as Reusable Highly Efficient Catalysts for a C_{sp3}–C_{sp3} Stille Coupling. *Angew. Chem. Int. Ed.* **2019**, *58*, 10330–10334.
(28) (a) Akram, M. O.; Banerjee, S.; Saswade, S. S.; Bedi, V.; Patil, N. T. Oxidant-Free Oxidative Gold Catalysis: The New Paradigm in Cross-Coupling Reactions. *Chem. Commun.* **2018**, *54*, 11069 − 11083; (b) Huang, B.; Hu, M.; Toste, F. D. Homogeneous Gold Redox Chemistry: Organometallics, Catalysis, and Beyond. *Trends Chem.* **2020**, *2*, 707 − 720; (c) Nijamudheen, A.; Datta, A. Gold-Catalyzed Cross-

Coupling Reactions: An Overview of Design Strategies, Mechanistic Studies, and Applications. *Chem. Eur. J.* **2020**, *26*, 1442 − 1487; (d) Kramer, S. Homogeneous Gold-Catalyzed Aryl–Aryl Coupling Reactions. *Synthesis* **2020**, *52*, 2017–2030.